

An improved constant current step-based grey wolf optimization algorithm for photovoltaic systems

Idriss Dagal^{a,*}, Burak Akın^{b,1} and Yaya Dagal Dari^{c,2}

^a*Yildiz Technical University, Electrical Engineering, Istanbul Turkey*

^b*Yildiz Technical University, Electrical Engineering, C-318 Davutpaşa Campus, Istanbul, Turkey*

^c*Institut National Supérieur des Sciences et Techniques d'Abéché (INSTA)*

Abstract. In this paper, an improved constant current step based on the grey wolf optimization (CCS-GWO) algorithm for photovoltaic systems is investigated. The development of grey wolf optimization has been widely spread over photovoltaic applications. This method is one of the metaheuristic swarm optimization algorithm groups inspired by an optimum means of chasing prey by grey wolves. The proposed technique applies constant current steps to the pack of wolves (alpha, beta, and omega) by monitoring the average of the internal current step and external current step in order to target the leader alpha wolf position. Moreover, the proposed technique solves the convergence process issues, low convergence speed, and premature local optima problems of the traditional GWO algorithm. This CCS-GWO algorithm accurately tracks the maximum power point from the photovoltaic systems for load charging in different partial shading conditions (PSCs). A number of standard benchmark functions are presented with low average cost functions and their corresponding standard deviation values. The simulation results revealed that the proposed CCS-GWO approach outperforms the existing GWO and GA algorithms in terms of efficiency (98.55%) and tracking time (0.3 s).

Keywords: Grey wolf optimization, metaheuristics, photovoltaics, maximum power point

1. Introduction

1.1. Background

The Grey wolf, salp swarm, artificial bees' colony, ant colony, and particle swarm are metaheuristic swarm optimization types. They are developed based on the behavior of organic colonies such as birds, fishes, bacteria, locusts, insects, and animals. In order to find an optimal solution for the PV system [1]

has developed a multi-grey wolf optimizer algorithm [2] has proposed a novel naturally inspired salp swarm-based grey wolf optimization maximum power point tracking (MPPT) to track rapidly and correctly the global maximum power point (GMPP) under stationary and varying partial shading conditions [3] has established a hybridization of grey wolf optimization-based fuzzy logic controller to catch and solve the GMPP and solve the oscillation problems around GMPP by tuning the generated output power at the GMPP [4] has exploited a new MPPT design utilizing the grey wolf optimization method for PV systems under partial shading conditions [5] proposed an improved grey wolf optimization algorithm with higher accuracy and faster convergence. For [6] in order to provide a better balance between

*Corresponding author. Idriss Dagal, Yildiz Technical University, Electrical Engineering, Istanbul Turkey. E-mail: idriss.dagal@std.yildiz.edu.tr; <https://orcid.org/0000-0002-2073-8956>.

¹<https://orcid.org/0000-0002-8647-1297>.

²<https://orcid.org/0000-0003-0373-0394>.

exploration and exploitation has created a modified grey wolf algorithm. The literature [7] proposed a novel grey wolf optimization (NGOW) algorithm to solve non-constrained problems of the optimization. In [8] a fuzzy logic variant of the hierarchical operator is used to improve the performance of the hierarchical GWO algorithm [9] used evolutionary population dynamics (EPD) in the grey wolf optimizer to considerably enhance the performance of the GWO algorithm in terms of local optima evasion, local search, convergence rate, and exploitation. In [10]. The literature review results on GWO revealed that the opportunities for creating more robust and stable variants of GWO still exist and will prevail over the weakness of current variants [11]. However, the traditional GWO method is susceptible to falling into local optimum, impacting the performance of the algorithm, thus an equalized grey wolf optimizer is developed with opposite learning (REGWO) to solve this issue. In [12], a grey wolf optimizer based on the levy flight algorithm and mutation mechanism has been achieved and the results illustrated better effectiveness and accurateness of the calibration of the proposed algorithm compared to other existing techniques [13], an improved hybrid grey wolf optimizer sine cosine algorithm (IHGWOSCA) is proposed with both training and testing highest accuracies of 93.33% and the lowest accuracies of 76.75% and 81.52% respectively.

1.2. Related work

The strong exploration technique of the grey wolf optimization (GWO) is used to update the followers' position to enhance the variance of the population [14, 15] proposed a grey wolf optimizer based on a dimensional learning strategy that experimental results reveal that the DLGWO has a good performance in solving the problem of global optimization. Moreover [16] used a cross-mutation grey wolf algorithm mostly to reduce the complexity of solving the spacecraft attitude maneuver problem and lessen the convergence time [17] introduced an extended adaptive grey wolf optimization (AGWO) algorithm in order to adjust the convergence of the three-point fitness convergence parameters and demonstrated the better performance of AGWO compared to the conventional GWO by decreasing the required number of iterations, therefore, it outperforms the existing GWO in terms of variants. Similarly, [18] developed an improved quasi-opposition learning and dynamic search based on the grey wolf optimization tech-

nique in order to solve the unbalance exploration and exploitation problem of the traditional GWO. Isaac et al. [19] designed a GWO algorithm that yields the same specific result achieved by the iterative-based sizing technique, the proposed method is faster in convergence as compared to the iterative approach. On the other hand, [20] discussed a modified bio-inspired approach with GWO that improves the effectiveness of the instruction detection system (IDS) in sensing both normal and abnormal traffic in the network. In the work [21], a grey wolf optimizer with bubble-net predation (GWO-BP) is used to solve the dynamic characteristics problem of the ordinary modeling technique, additionally, the GWO-BP effectively balances the sensing and exploitation capabilities to quickly meet the optimum value and enhances the accuracy. Likely [22], combined GWO and an improved Gaussian diffusion method to enhance the accuracy of the source term estimation (STE) [22]. The feature selection for classification issues based on the wrapper approach was solved by a new grey wolf optimizer algorithm incorporated with a two-phase mutation [23, 24]. This research proposes a renowned nature-inspired flower pollination algorithm (FPA) which is intensely reviewed, modified, and integrated with the arbitrary walk filter to enhance its performance in terms of tracking speed, and efficiency [25]. The efficiency, accuracy and tracking speed of FPA algorithm is optimized. Evaluation of the proposed OFPA (Optimized Flower Pollination Algorithm) and the old FPAs technique is achieved for null shading condition, poor PSC, powerful PSC, and varying weather conditions [26] subsection adaptive hill climbing method (SSAHC), for getting the maximum power point (MPP) of a photovoltaic (PV) solar panel for any temperature and solar radiation level is proposed [27]. Reduce and Fix method is positively presented as enhancement in PAO algorithm to mitigate these issues of tracking speed and oscillations [28]. The proposed optimized hill climbing (OHC) algorithm achieves null steady-state oscillations without cooperating with the strength of the conventional hill climbing algorithm. They applied both algorithms to an off-grid PV system under constant and varying weather conditions, and the results show the superiority of the proposed OHC algorithm over the traditional HC algorithm. Numerous maximum power point tracking methods often stand out and set the partial shading conditions. However, depending merely on the algorithm reveals several advantages and shortcomings with problems like non-speedy

tracking to global maximum power (GMP), failure of tracking path, extensive oscillations around GMP.

This paper is outlined as follows: Section 1 presents the modeling and description of the proposed CCS-GWO system; Section 2 discusses mathematical modeling and implementation of the proposed algorithm, while Section 3 includes the discussion and results of the simulation. Finally, Section 4 covers the conclusion including the findings of the study.

1.2.1. Research gap and contribution

An improved GWO [52] is proposed to enhance wolf agents' global and local research ability by using the Gaussian distribution function and nonlinear convergence technique [53] proposes an evolution and elimination method based on GWO in order to perform a good matching between the exploitation and exploration, further hasten the convergence and boost the conventional GWO accuracy. GWO has great potential for solving optimization issues in various disciplines of study [54]. However, It presents some shortcomings such as low convergence speed and local optima stagnation. Therefore, [55] suggests a new GWO with variable weights (VW-GWO) that reduces the possibility of being stuck in local optima, and [56] introduces a new 2DP colonies model embedded with a blackboard in order to empower the simulation of the grey wolf algorithm. In the same perspective, [57] works on the multi-objective grey wolf optimization by using several UCI datasets for attribute reduction. In [58], a fitness based on GWO is used to overcome the manual classification of spam reviews and obtain the optimal cluster heads [59] investigates an inspired GWO approach that expands the traditional GWO by means of a nonlinear adjustment method and a new position-updating equation. In order to improve the global research and local research ability of the existing GWO, [60] implemented a new algorithm with a convergence factor based on S-function change. Multi-objective optimization is used to increase the scheduling performance as compared to the single objective function [61].

The following are the proposed CCS-GWO algorithm contributions:

- The proposed technique can be easily applied in PV solar applications where GMPP is required.
- In order to hunt the prey, the wolf's mutation (movement steps) is improved, that is to say the exploration of the GWO becomes accurately effective.

- The proposed CCS-GWO method successfully tracks the required power with minor tracking time by using the adjacent or sequencing way of combined internal and external steps.
- The conventional GWO fails to yield during the converging process, and besides its regular problems such as convergence speed and local optimum stagnation, therefore, the proposed CCS-GWO series or adjacent combination of both internal and external step techniques mitigates the current problems mentioned.

1.3. System modeling

1.3.1. System description

The proposed CCS-GWO technique combines the PV-shaded arrays interfaced with the load through a boost converter. The boost converter is used to examine the PV array's voltage. The CCS-GWO algorithm is used to check on the global power by controlling the boost converter's duty cycle by means of the driver circuit Fig. 1.

1.3.2. System components modeling

1.3.2.1. Modeling of photovoltaic solar panel. The equivalent circuit of a PV solar module consists of one of several diodes, parallel and series resistors [37]. The leakage current flow is minimized by the parallel resistor. The series resistor plays the role of measuring losses. PV solar cell presents two models: the single-diode model (Fig. 2) and the double-diode model. The single diode model has five parameters in Equation (1). The double diode model is more accurate as compared to the single diode model; however, it requires additional parameters in order to successfully model the PV solar cell. Due to its simplicity, the single diode model (Fig. 2) is used and presented some parameters such as photocurrent (I_L), output voltage (V), dark saturation current (I_0), electron charge (q), Boltzmann constant (K), ideality factor (A), absolute temperature (T), the series resistor (R_S) and the parallel resistor (R_{SH}). Equations (1), (2), (3), and (4) are approximative open circuit voltage, short circuit current, and open voltage for the PV solar cell I-V characteristics respectively [62–64].

$$I = I_L - I_0 \left\{ \exp \left[\frac{q(V + IR_S)}{nkT} \right] - 1 \right\} - \frac{V + IR_S}{R_{SH}} \quad (1)$$

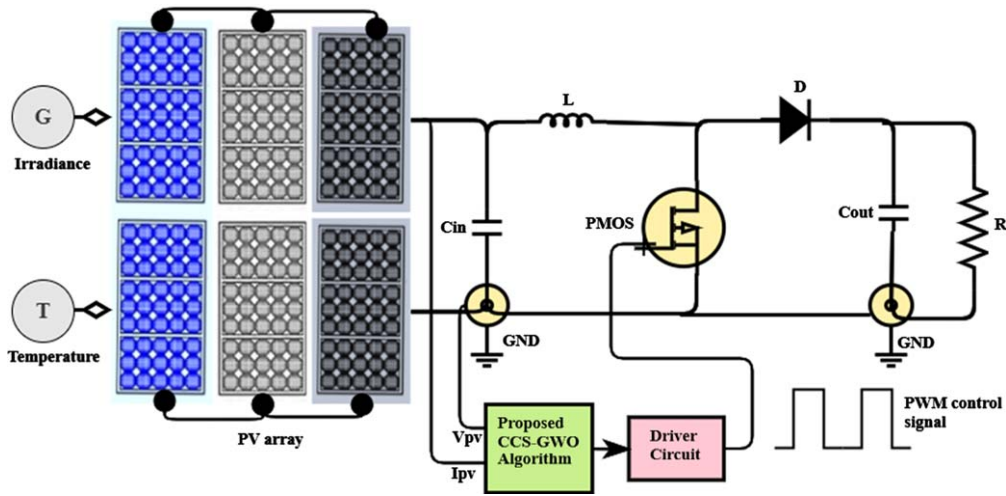


Fig. 1. Circuit block diagram.

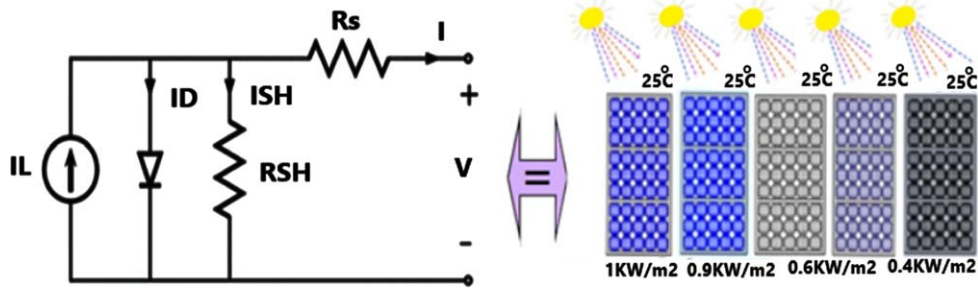


Fig. 2. Circuit of Solar panel and its equivalent panels series.

Through, the semiconductor material and solar panel, the resistance R_S are offered. Complexity exists in describing the shunt resistance R_{SH} . For the p-n junction of non-ideal nature, a short circuit path is given around the junction due to the presence of the impurities located near the cell edges. In an ultimate case, R_S is 0, whereas R_{SH} is infinite. To improve the products, the manufacturers tried to minimize the resistance effect. Similarly, the ultimate setup is not possible.

The R_{SH} outcome is not considered. R_{SH} is infinite for simplification, thus Equation (1) the last term is abandoned.

1.3.2.2. Open circuit voltage and short circuit current of PV solar panel. Dual significant current-voltage points are the short-circuit current I_{SC} , and the open-circuit voltage V_{OC} .

The power generation is 0 at both points. From (1) V_{OC} can be approximated when $I=0$, the R_{SH} is discarded shown in Equation (2) the I_{SC} is at $V=0$

and nearly the same as the light generated current I_L shown in Equation (3).

$$V_{OC} \approx \frac{nkT}{q} \ln \left(\frac{I_L}{I_0} + 1 \right) \tag{2}$$

$$I_{SC} \approx I_L \tag{3}$$

By means of the solar circuit, the maximum power is generated at MPP and the current-voltage characteristics which are distinctive at various temperatures are shown in following Fig. 3.

1.3.2.3. Impact of irradiance and temperature. The crucial environmental factors such as temperature and irradiance require paramount consideration. PV solar panel P-V and I-V characteristics subjected to these factors present a significant variation in terms of values. In daily climate change, the maximum power point changes, and due to that, some means of MPP tracking are continually obliged to guarantee the maximum requested power drawn from the PV

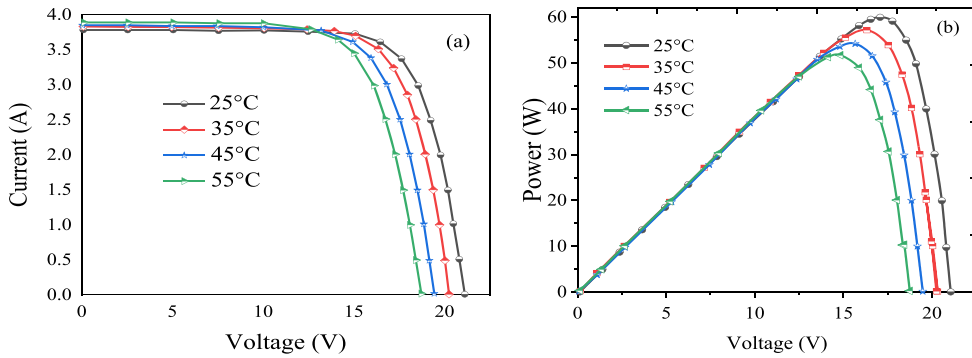


Fig. 3. Solar panel characteristics I-V (a) and P-V (b) curve at constant irradiation and varying temperatures.

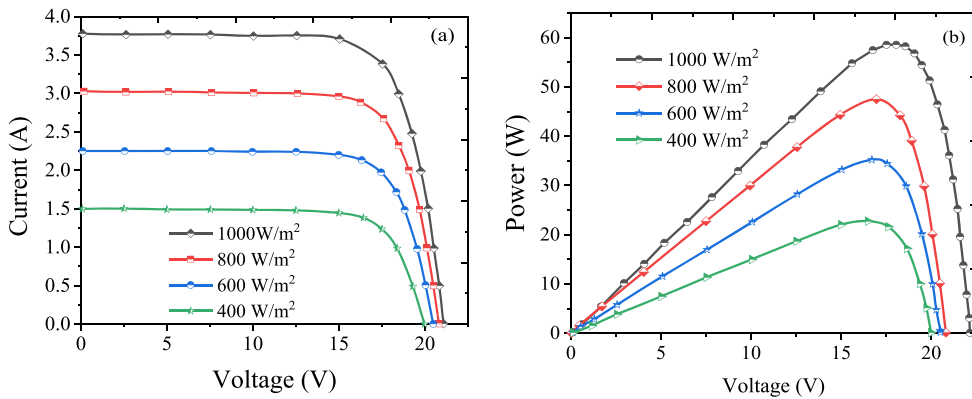


Fig. 4. V-I (a) and P-V (b) curve at four irradiance variations and constant temperature.

solar panel. Figure 4 shows the PV panel’s V-P and V-I characteristics curves which are exposed to the effects of the irradiance.

Figure 4 depicted that by comparing with voltage, the change in current is greater. The dependency of voltage on irradiation is frequently abandoned. When the irradiation rises from the positive value of the current and the voltage, the power is also positive. Thus, more power is generated when more irradiation is available.

On the contrary, the voltage is affected mostly by temperature. The open-circuit voltage is linearly dependent on the temperature, as shown in Equation (4).

$$V_{OC} = \frac{nkT}{q} \ln \left(\frac{I_{SC}}{I_0} + 1 \right) \quad (4)$$

Based on Equation (4) the temperature effects on V_{OC} show negative value since the voltage decreases when the temperature increases. The little increase in current doesn’t compensate for the voltage decrease due to the rise in temperature and thus a reduction

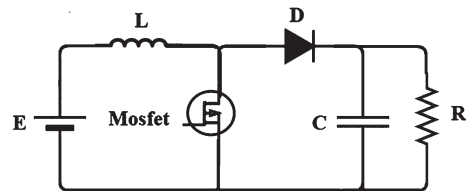


Fig. 5. Boost converter.

in power is seen. When the temperature changes, the higher power point, short circuit current, and open-circuit voltage vary.

1.3.2.3. Boost converter. The conventional boost converter circuit diagram is shown in Fig. 5. The role of the boost converter is to step up the input voltage. It is comprised of the main power switch, a semiconductor diode switch, an inductor, and an output capacitor. The boost converter has two modes of operation.

In the on-state, the main power switch is closed or switched on, the diode switch is reverse-biased, and

the induction is charged from the power supplied by the capacitor. At that state, no current flows to the load, and only the capacitor feeds the load.

In the off state, the main power switch is opened or switched off, the diode switch is forward-biased, and the capacitor gets fully charged by the power stored in the inductor via the diode switch [65, 66].

The input voltage and output voltage relationship

$$V_0 = \frac{1}{1-D} V_{in} \text{ with } D \text{ the duty cycle} \quad (5)$$

The peak-to-peak inductor ripple current is deduced as follows:

$$\Delta i_L = D(1-D) \frac{V_0}{f_p L} \quad (6)$$

The input current and output current relationship.

$$I_{in} = \frac{1}{1-D} I_0 \quad (7)$$

The peak-to-peak output ripple voltage is expressed as follows.

$$\Delta V_0 = \frac{1}{f_p C} D I_0 \quad (8)$$

2.2.1. Grey Wolf Optimizer (GWO)

Grey wolf optimization is predatory behavior of the population-based metaheuristic type algorithm. The GWO comprises four populations working on an orderly leadership hierarchy. In the pack, they collaborate together for three major steps such as hunting, encircling, searching, and attacking the prey. GWO population has four levels α , β , δ , and ω ranking first, second, third, and fourth respectively. In Fig. 6, the grey wolves are located as α , β , δ , and ω from the top layer to the bottom layer respectively in their hierarchical activity manner. The α grey wolf is the utmost chief of the pack, this grey wolf gives the most important decisions such as hunting, lunchtime, bedtime, rest time, wake-up time, and so on. The β grey wolf represents the deputy of the α grey wolf and acts as the adjunct of the alpha grey wolf and after the death of the α grey wolf, the β grey wolf can ensure the same responsibilities done by the alpha wolf. In the third hierarchy, the δ grey wolf is ordered to follow the instructions of the alpha and beta grey wolves. The δ grey wolf leads the omega grey wolf. The ω grey wolf is the last ordered grey wolf, which obeys hierarchically to all the grey wolves. GWO system position updating is depicted in Figs. 6 and 7 respectively.

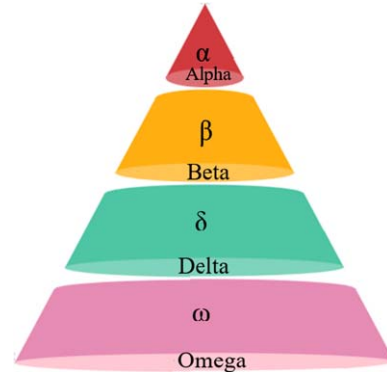


Fig. 6. Hierarchy of wolves with dominance decreases from the top to down (α , β , δ , and ω).

2.2.2. History of grey wolves live

2.2.2.1. Inspiration. They live in packs of four to nine groups and that can vary based on their ancestors. Wolves have body language communication like bees. Barking and howling are used for warning long-distance communication respectively. A wolf used to challenge its travel companion by growling or laying its ears back on its head. In the group, there are male and female hierarchies. The Grey wolves are of four different types namely alpha, beta, delta, and omega. The most dominant over the entire pack is the male alpha grey wolf type. The alpha male and male-only has babies that breed. At the age of three, the young wolf becomes a teenager and joins the pack or leaves for hundreds of miles to find its own land. At birth, their pups can't see or hear and approximately weigh one pound. They work on a strict socially dominant hierarchy.

- The alpha is mainly chief for making decisions like hunting, sleeping, time to search for place and so for. The (alpha) wolves are not absolutely the strongest members of the pack, but they are the best in terms of controlling the pack.
- The beta wolves are second in the hierarchy of grey wolves; they are subordinate or deputy wolves after alpha wolves and help alpha wolves in decision-making or other events. Beta wolves can replace or lead if one of the alpha wolves passes away, becomes sick, is seriously wounded, or is too old. The respect is tensed up to alpha wolves, but they (beta wolves) give authority to other lower-level wolves as well. They are considered as counselors to the alpha wolves and punishment givers to the others.

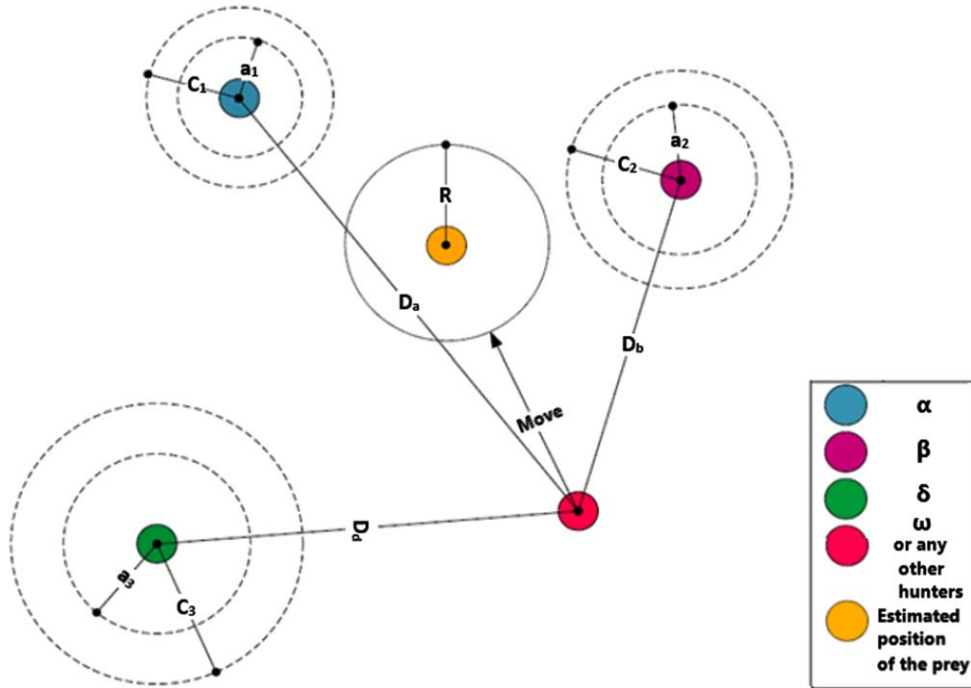


Fig. 7. Position updating in grey wolf optimization (GWO) system [14].

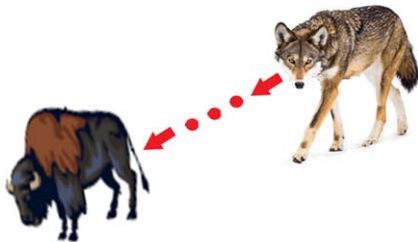


Fig. 8. Physical images of the grey wolf and its prey.

- Omega are the lowest ranking wolves, act as scapegoats, they are the weakest wolves, and in a hierarchal manner, they eat after all the wolves that live in the pack, they are sometimes babysitters in the pack.
- The delta wolves are called subordinate because they must submit to alpha and beta wolves but, on other hand, they dominate omega wolves. The grey wolf and the prey are shown in Fig. 8 below.

2.2.2.2. *Mathematical modeling and the proposed algorithm.* In this section, the mathematical modeling of the grey wolves' hunting strategy, social behavior, chasing, encircling, tracking, and attacking prey are investigated in order to improve the implementation of the grey wolf optimizations.

2.2.2.3. *Social hierarchy.* In the mathematical modeling of the social behavior of wolves when applying GWO, we considered alpha as the first best solution. Beta and delta are the second and third-best solutions respectively. The omega wolf is the rest and the last candidate to be presented. The hunting event of the GWO is conducted by α , β , and δ whereas, the ω wolves follow these three wolves [67].

2.2.2.4. *Encircling or blockading prey.* The grey wolves encircle or blockade prey during the hunt. The following Equations are proposed for the mathematical modeling [68–70].

$$\vec{D} = \left| \vec{C} \cdot \vec{X}_P(t) - \vec{X}(t) \right| \quad (9)$$

$$\vec{X}(t+1) = \vec{X}_P(t) - \vec{A} \cdot \vec{D} \quad (10)$$

Where t indicates the current position, \vec{X}_P is the position of the prey, and \vec{X} presents the position vector of a grey wolf. \vec{A} and \vec{C} are coefficient vectors calculated as follows [69, 71].

$$\vec{A} = 2\vec{a} \cdot \vec{r}_1 - \vec{a} \quad (11)$$

$$\vec{C} = 2 \cdot \vec{r}_2 \quad (12)$$

Where components \vec{a} are linearly decreased from 2 to 0 over the course of iterations and \vec{r}_1, \vec{r}_2 are random vectors in [0,1].

$$\vec{a} = 2 - 2 \left(\frac{it}{\max \text{ iterations}} \right) \quad (13)$$

2.2.2.5. Hunting. Grey wolves have a high ability to identify the prey's position and encircle them in their location. The alpha grey is the guidance herd to lead others in their hunting activities. However, beta and delta wolves may also participate in hunting too. In the conceptual space, we do not have any remote idea about the location of the optimum prey. While mathematically mimicking the hunting behavior of the grey wolves, alpha, beta, and delta are deemed to have excellent knowledge about the probable location of the prey. Therefore, the first three best solutions have been found to date so far and kept. The rest of the search candidates, including omega wolves, are compelled to alter their positions corresponding to the position of the best search agent. These equations are proposed in order to achieve the hunting process [67, 72, 73].

$$\begin{aligned} \vec{D}_\alpha &= \left| \vec{C}_1 \cdot \vec{X}_\alpha - \vec{X} \right|, \vec{D}_\beta = \left| \vec{C}_2 \cdot \vec{X}_\beta - \vec{X} \right|, \\ \vec{D}_\delta &= \left| \vec{C}_3 \cdot \vec{X}_\delta - \vec{X} \right| \end{aligned} \quad (14)$$

$$\begin{aligned} \vec{X}_1 &= \vec{X}_\alpha - \vec{A}_1 \cdot (\vec{D}_\alpha), \vec{X}_2 = \vec{X}_\beta - \vec{A}_2 \cdot (\vec{D}_\beta), \\ \vec{X}_3 &= \vec{X}_\delta - \vec{A}_3 \cdot (\vec{D}_\delta) \end{aligned} \quad (15)$$

$$\vec{X}(t+1) = \frac{\vec{X}_1 + \vec{X}_2 + \vec{X}_3}{3} \quad (16)$$

2.2.2.6. Attacking prey (exploitation). The grey wolves start their mission of attacking when the prey stops moving. In order to mathematically achieve this step, we decrease the value \vec{a} that makes the range of \vec{A} also decreases Equation (11). Due to the range of \vec{A} $[-\vec{a}, \vec{a}]$. Therefore, the value of \vec{a} is decreased from 2 to 0 over the iteration chain, and that makes the range of $|\vec{A}| < 1$, and forces the wolves to attack the prey.

2.2.2.7. Searching for prey (exploration). The searching process of the wolves mostly depends on the movements or the position of alpha, beta, and delta wolves to look for the prey in a diverging

manner and, they attack the prey in a converging way. In the divergence case, the mathematical modeling is done by using random values of $|\vec{A}| > 1$ or $|\vec{A}| < -1$ to force the search agent to move away (diverge) from the prey. The exploration situation is applied in this case and allows the grey wolf optimization (GWO) algorithm to word widely explore the prey. C is another prominent factor in exploration. It is very helpful especially during the final iterations in case the local minimum stagnation problem occurs. \vec{C} with values range in [0,2] can be considered as an obstruction effect to approach prey in the natural world. This obstacle or obstruction in nature generally happens during the hunting period of wolves and that precludes them from swiftly and accurately approaching their prey.

2.2.2.8. Proposed CCS-GWO Algorithm and its pseudo coding. The proposed CCS-GWO algorithm works based on the search agents' or candidates' movement or position steps. As far as the alpha grey wolf is the leading and decision maker herd, the step mutations are applied to alpha, beta, and delta successively in that order.

The descriptive explanation of the proposed CCS-GWO algorithm based on internal and external steps techniques is as follows.

The steps are divided into two steps:

- First step is called the internal step or lower step, and the second step is denoted by the external step or upper step.
- For $|\vec{A}| < 1$, where the wolves are converging toward the prey, the internal step is appropriately applied and the wolves achieve their mission whereas, the external step fails from being applied in this case.
- For $|\vec{A}| > 1$, where the wolves diverge away from the prey, the internal step fails from being applied and the wolves did not achieve their mission, whereas the external step is successfully applied, and the wolves reach their prey.
- Both $|\vec{A}| < 1$, and $|\vec{A}| > 1$ cases: This case is called the hesitating or doubting step.

During the doubting step, when both are applied simultaneously in adjacent and parallel manners, the wolves fail to reach their target prey and the results are depicted in Fig. 17 (a) and 17 (b) respectively.

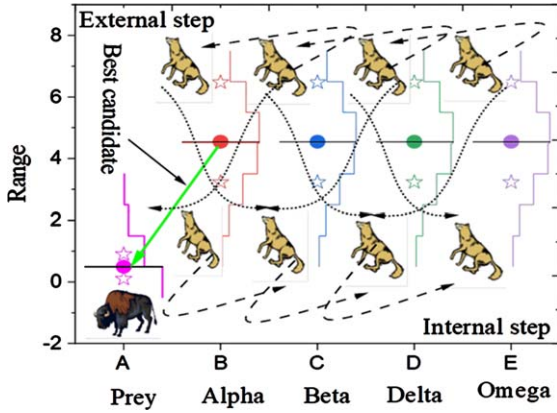


Fig. 9. Pictorial view of grey wolves' hierarchy strategies.

When both steps are applied intermittently in an adjacent manner, the wolves successfully reach their target prey, and the results are presented in Fig. 14 (a) and 14 (b).

If the intermittent adjacent manner is applied and the internal step is dominant, therefore, the result is shown in Fig. 15 (a).

If the intermittent adjacent manner is applied and the external step is dominant, therefore, the result is shown in Fig. 13 (a) and 13 (b).

The simultaneous parallel manner with the internal step dominant is illustrated in Fig. 16 (b).

The Parallel manner cannot be applied for both intermittent steps, only the adjacent manner is applicable in this case. Figure 9 gives an illustrative view of the hierarchical strategies of the proposed technique.

The modified mathematical expressions of the new updated hunting process are expressed as follows.

$$\begin{aligned}
 WolfPosition(is, es) &= \left(\frac{X_1 + X_2 + X_3}{3}\right) is + \left(\frac{X_1 + X_2 + X_3}{3}\right) es \\
 &= \left(\frac{X_1 + X_2 + X_3}{3}\right) (is + es) \tag{17}
 \end{aligned}$$

$$X_1 = X_\alpha - A_1 (D_\alpha is + D_\alpha es) \tag{18}$$

$$X_2 = X_\beta - A_1 (D_\beta is + D_\beta es) \tag{19}$$

$$X_3 = X_\delta - A_1 (D_\delta is + D_\delta es) \tag{20}$$

$$D_\alpha i + D_\alpha e = |C_1 \cdot X_1 - WolfPosition(is, es)| \tag{21}$$

$$D_\beta is + D_\beta es = |C_2 \cdot X_2 - WolfPosition(is, es)| \tag{22}$$

$$D_\delta is + D_\delta es = |C_3 \cdot X_3 - WolfPosition(is, es)| \tag{23}$$

With *is* and *es* denoted by internal step and external step respectively.

The steps progress Fig. 10 of the proposed algorithm is described as follows.

- Step 1: Initialize the population positions of *n* grey wolves $X(is, es) = 1, \dots, n$.
- Step 2: Initialize the parameters *a*, *A*, and *C*
- Step 3: Compute the fitness of each grey wolf in internal and external step position.
- Step 4: Assign the best grey wolves to *X_{alpha}*, *X_{beta}*, and *X_{delta}* respectively.

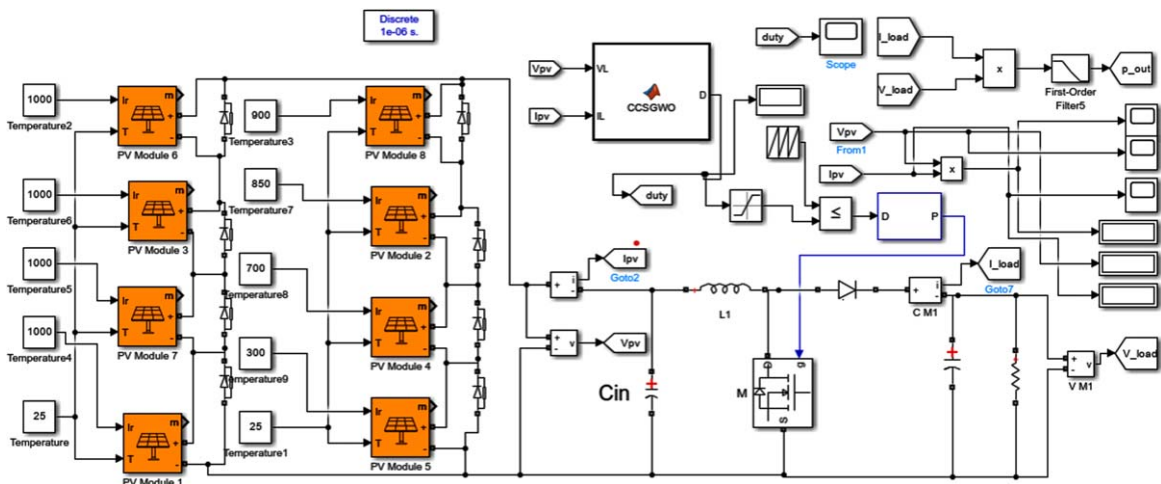


Fig. 10. The proposed CCS-GWO algorithm MATLAB implementation.

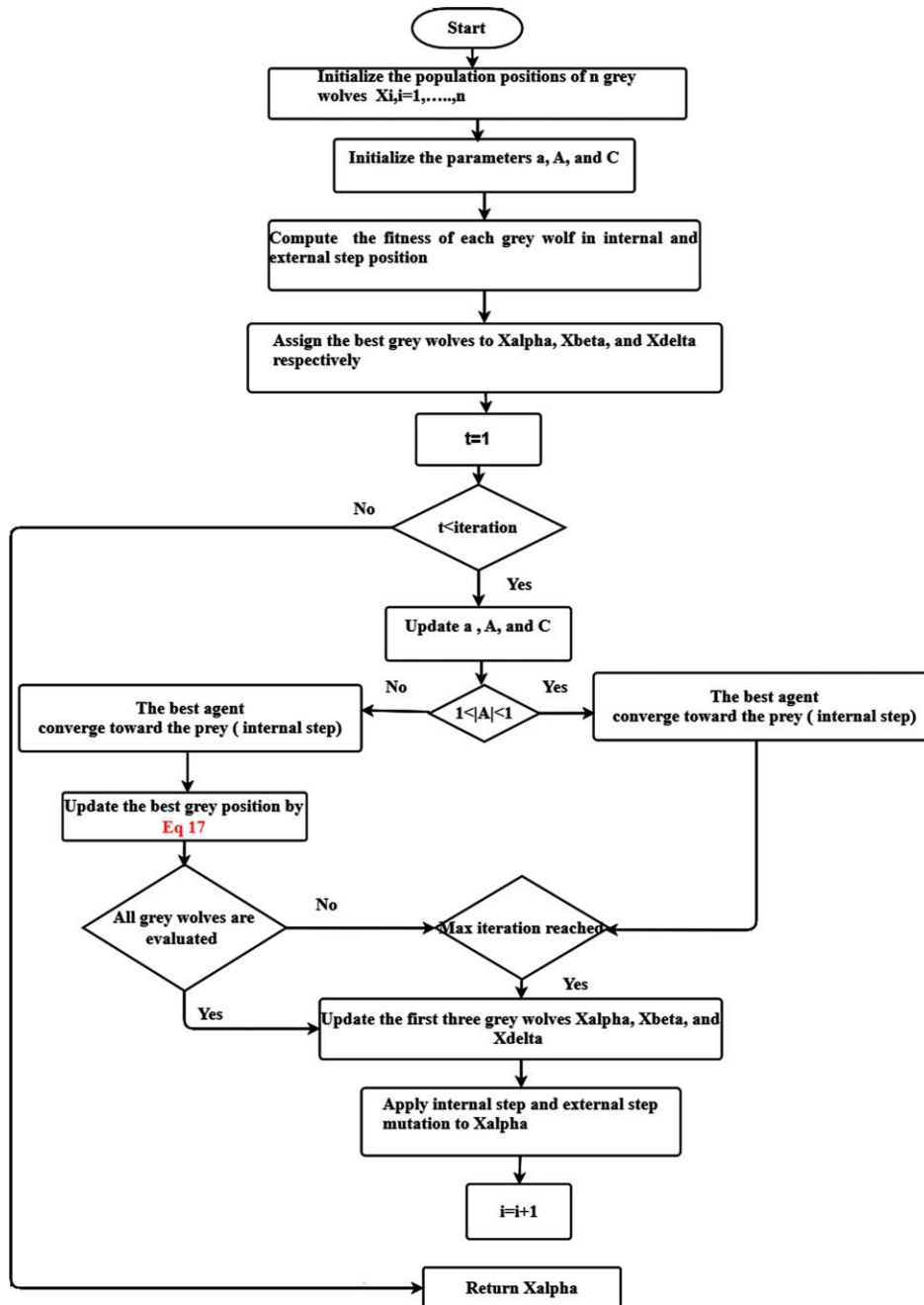


Fig. 11. The Proposed CCS-GWO Algorithm and Pseudocode.

Step 5: Define $t = 1$
 Step 6: While ($t < \text{iterations}$) for each grey wolf
 Step 7: Update the position of the current grey wolf using Equation (17)
 Step 8: End for
 Step 9: Update a , A , and C

Step 10: While ($1 < |A| < 1$)
 Step 11: If $A < 1$, the best agent converges toward the prey (internal step)
 Step 12: If $A > 1$, the best agent diverges from the prey (external step)
 Step 13: Check whether all the agents are evaluated.

Step 14: Verify whether the maximum iteration is reached.

Step 15: Update the first three grey wolves Xalpha, Xbeta, and Xdelta

Step 16: Apply internal step and external step mutation.

Step 17: Define $i = i + 1$

Step 18: End while

Step 19: Return the best grey wolf Xalpha.

In order to understand some amalgams on the best fitness value of an algorithm, it is not obvious that they can be detected with a single objective function, this is the reason why we prefer to prove the accuracy and performance of the proposed CCS-GWO method by using different functions such as unimodal bench function, multimodal bench function, and fixed dimension multimodal bench function (Table 1). For each bench function, the number of search agents and the maximum number of iterations are 30 and 150 respectively. In Table 1, the proposed CCS-GWO algorithm presents the bench functions $F5=(0.07265, 0.01993)$, $F11=(0.03694, 0.01213)$, $F19=(0.03653, 0.01331)$ as the average cost function and the corresponding standard deviation (std) results respectively. These bench functions permit to compute the exploitation capability of the proposed technique.

3. System description under analysis

Different case studies have been conducted to assess the effects of uniform irradiance, fast varying irradiance, temperature, partial shading condition, load type and frequency. Besides, a comparative study of different algorithms was also presented.

3.1. Results and analysis

In order to validate and prove the accuracy of the proposed study, we choose under partial conditions 4S2P for the MSX-60 W panel subjected to two patterns $G1 = [1000, 1000, 1000, 1000]$ and $G2 = [900, 850, 700, 300]$ at 25°C [74] Fig. 12 (a) and 12 (b) considered as the inputs of this study with global maximum power 345 W and current 7 A respectively.

Based on the above Fig. 12 (b) input applied to the proposed CCS-GWO technique, we observe the followings results depicted Fig. 13 (a) and 13 (b). In Fig. 13 (a), the result shows that the CCS-GWO accurately tracked the current at a low tracking time of 0.5 s, moreover, the internal step and external step curves also follow-up with the CCS-GWO curve. In Fig. 12 (b), the result indicates that the genetic algorithm based constant current step (GA-CCS) tracks the current at a tracking time of 16,05 s and both inter-

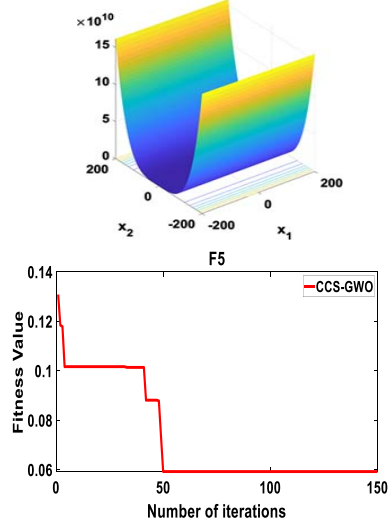
Table 1
Comparative results of GWO, hybridization and MPPT computing methods

MPPT Techniques	Tracking efficiency	Tracking Speed	Oscillation around MPP	Tracking ability under PSCs	Convergence speed	Implementation Complexity
[29]	Medium	Fast	Small	High	Medium	Medium
[30]	Medium	Fast	Small	High	Medium	High
[31]	Medium	Fast	Small	High	Medium	High
[32]	Medium	Fast	High	Poor	High	Medium
[33]	High	Fast	Small	High	High	High
[34]	High	Fast	Small	High	Medium	High
[35]	Medium	Fast	Small	High	High	High
[36]	High	Fast	Small	High	Medium	High
[37]	High	Medium	Small	High	High	High
[38]	High	Fast	High	High	Very High	High
[39]	High	Fast	Small	High	High	Medium
[40]	High	Fast	Small	Poor	High	High
[41]	High	Fast	Small	Poor	High	Medium
[42]	Medium	Fast	Small	Poor	Medium	Medium
[43]	Medium	Fast	Small	High	High	Low
[44]	High	Fast	Small	High	High	Medium
[45]	High	Fast	Small	High	Medium	Medium
[46]	Medium	Fast	Small	High	Medium	High
[47]	High	Fast	Small	High	High	High
[48]	Medium	Fast	Small	High	High	Medium
[49]	Medium	Fast	Small	High	High	Medium
[50]	Medium	Fast	Small	High	High	Medium
[51]	High	Fast	Small	High	High	Medium

Table 2
Bench functions and parameters spaces of the proposed CCS-GWO Algorithm

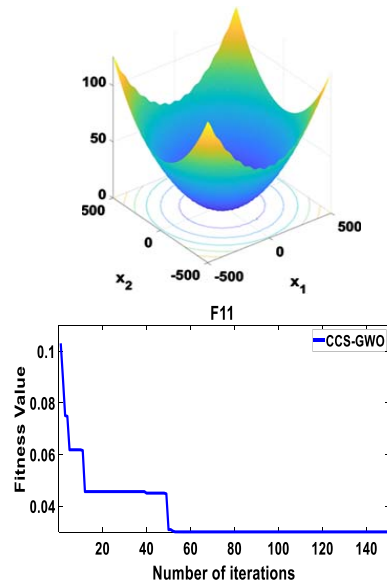
Unimodal bench function

$$f_5 = \sum_{i=1}^{n-1} \left[100(x_{i+1} - x_i^2)^2 + (x_i - 1)^2 \right]$$



Multimodal bench function

$$f_{11} = \frac{1}{400} \sum_{i=1}^n x_i^2 - \prod_{i=1}^n \cos \frac{x_i}{\sqrt{i}} + 1$$



Fixed dimension multimodal bench function

$$f_{19} = - \sum_{i=1}^4 c_i \exp \left(- \sum_{j=1}^3 a_{ij} (x_j - p_{ij})^2 \right)$$

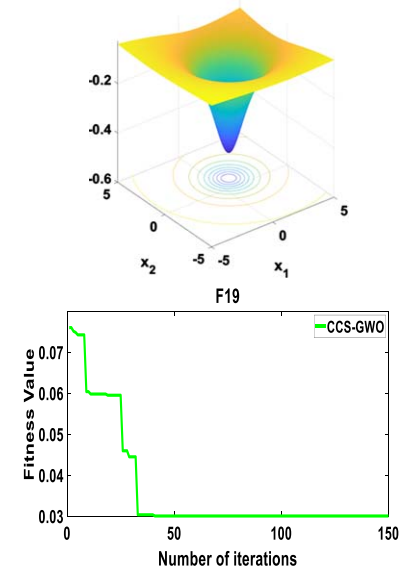


Table 3
Boost converter PV solar panel and algorithms parameters setting

Boost converter parameters		Selected PV solar panel parameters			
Switching Frequency ($F_{sw} = 50 \text{ KHz}$)	P_{max}	V_{max}	V_{oc}	I_{max}	I_{sc}
Inductance ($L = 850 \mu H$)	60 W	17.1 V	21.1 V	3.5 A	3.8 A
Capacitance ($C = 220 \mu F$)					
Duty cycle ($D_{min} = 0.1$ & $D_{max} = 0.9$)					
Load ($R = 10 \Omega$)					
CCS-GWO		GWO		GA	
Number of populations 200		Number of populations 200		Number of populations 200	
Number of iterations 5		Number of iterations 5		Number of iterations 5	
Convergence factor 2-0		Convergence factor 2-0		Crossover probability 0.8	
Internal step [-1,1]				Mutation probability 0.1	
External step [-1,1]					

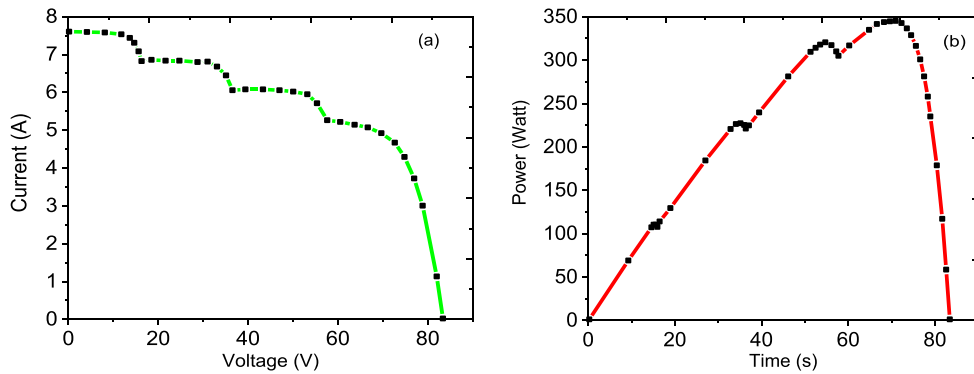


Fig. 12. PV module P-V curve (a) and I-V curve (b) under partial shading conditions.

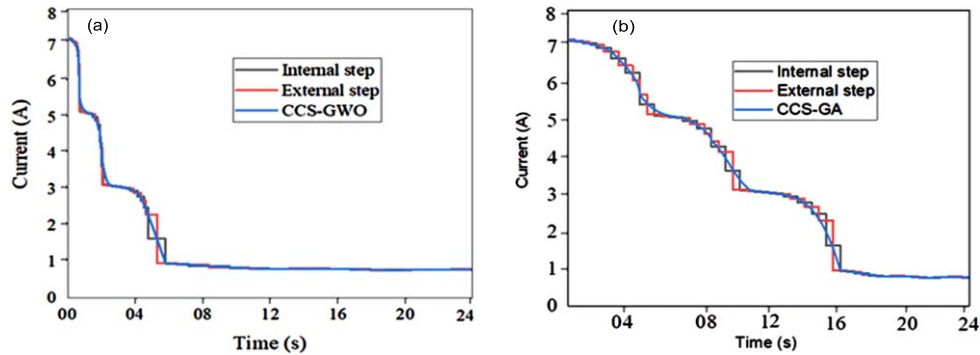


Fig. 13. CCS-GWO, internal and external step curves (a) and CCS-GA, internal and external step curves (b) under partial shading conditions.

nal and external steps fail to follow up with CCS-GA from 0 to 16,05 s.

In this study, we presents two results:

For Fig. 15 (a), the Standard Test Conditions (1000 W/m^2 , 25°C) is applied and the CCS-GWO, internal and external step power curves are shown. The adjacent internal and external steps method is used and CCS-GWO smoothly tracks the global maximum power of 345 W at a tracking time of 5 s.

For Fig. 15 (b), the CCS-GWO, internal and external step power curves are depicted and subjected to two patterns $G1 = [1000, 1000, 1000, 1000]$ and $G2 = [900, 850, 700, 300]$ at 25°C Fig. 12 (a) under partial conditions 4S2P. The result reveals that by using the adjacent internal and external steps method, the CCS-GWO curve starts from 01 s (due to step mutation) and tracks the global maximum power of 345 W at a tracking time of 5 s.

Table 4
Efficient and powers of different algorithms under PSCs and STC

Solar irradiance [W/m ²]	Temperature [°C]	Weather conditions		Algorithms					
		STC	PSC	CCS-GWO		GWO		GA	
				P_{GMPP}	Eff	P_{GMPP}	Eff	P_{GMPP}	Eff
1000 900	25	✓		349	99.83	343	98.81	341	97.85
1000 850									
1000 700			✓	340	99.77	336	98.74	326	97.73
1000 300									
1000 900	45	✓		335	99.69	330	98.63	309	97.47
1000 850									
1000 700			✓	325	99.51	321	98.44	302	97.33
1000 300									

Table 5
Comparison with other algorithms

Type	CSS-GWO	GWO	GA
Tracking speed	Fast	Medium	Slow
Tracking accuracy	Accurate	Accurate	Low
Design complexity	Medium	Medium	Low
Steady state oscillation	Zero	Less	Less
Convergence/limitations	Global peak	Local peak	Local peak
Computational time/speed	1.94S	2.45S	2.89S

3.2. Proposed CCS-GWO algorithm accuracy and efficiency

We analyze the efficiency and accuracy of CCS-GWO, GWO and GA under different partial shading conditions by altering the irradiance and temperature. The efficiency values as seen in Table 4 were calculated by means of Equation (24) which is defined as the ratio of the tracked output power to the existing maximum power of the system at the PV input. A comparison of the proposed algorithm with other existing techniques based on accuracy, efficiency, complexity, oscillation, and limitation is presented in Table 5.

$$\eta = \frac{P_{out_{tr}}}{P_{in_{pv}}} \times 100 \quad (24)$$

With $P_{out_{tr}}$ tracked output power and $P_{in_{pv}}$ maximum available power to the PV input.

Figure 14 (a), (b) and (c) are histogram representation of worst, average and best cases of CCS-GWO, GWO and GA algorithm respectively.

The mean accuracy of GA algorithm is 72%, the GWO has the mean accuracy of 78.7% whereas the proposed CCS-GWO outperforms the two other algorithms with a mean accuracy of 93%.

In this part, both Fig. 16 (a) and 16 (b) are simulated under complex partial shading conditions (CPSCs) and the results have proved that the proposed CCS-

GWO algorithm demonstrates higher performance and good accuracy as compared to the conventional GWO with tracking times of 15 s and 17 s respectively.

Here, Fig. 17 (a) and 17 (b) show GWO same curves in different aspects:

Figure 17 (a) shows that the CCS-GWO is in dominance mode because by applying the adjacent internal and external step method, from the starting until the end of the path, the CCS-GWO curve is above that of internal-external step curves. In contrast, the non-dominance mode has been found in Fig. 15 (a) where the CCS-GWO curve is under that of internal-external steps one.

Figure 17 (b) presents the GWO curves under normal, partial shading and internal-external steps conditions. The CCS-GWO demonstrated a good tracking time as compared to the normal and partial shading conditions.

This part presents comparative curves of GA, GWO and CCS-GWO Fig. 18 (a) and CCS-GWO, internal step and external step curves Fig. 18 (b).

Figure 17 (b) shows that the external step is dominant (adjacent mutation step mode) as compared to the internal step because the CCS-GWO curve is mostly close to the external step curve.

Figure 19 shows that both adjacent mutation step mode curve (a) and parallel mutation step mode (b) are dominant because internal-external step curves are above the CCS-GWO.

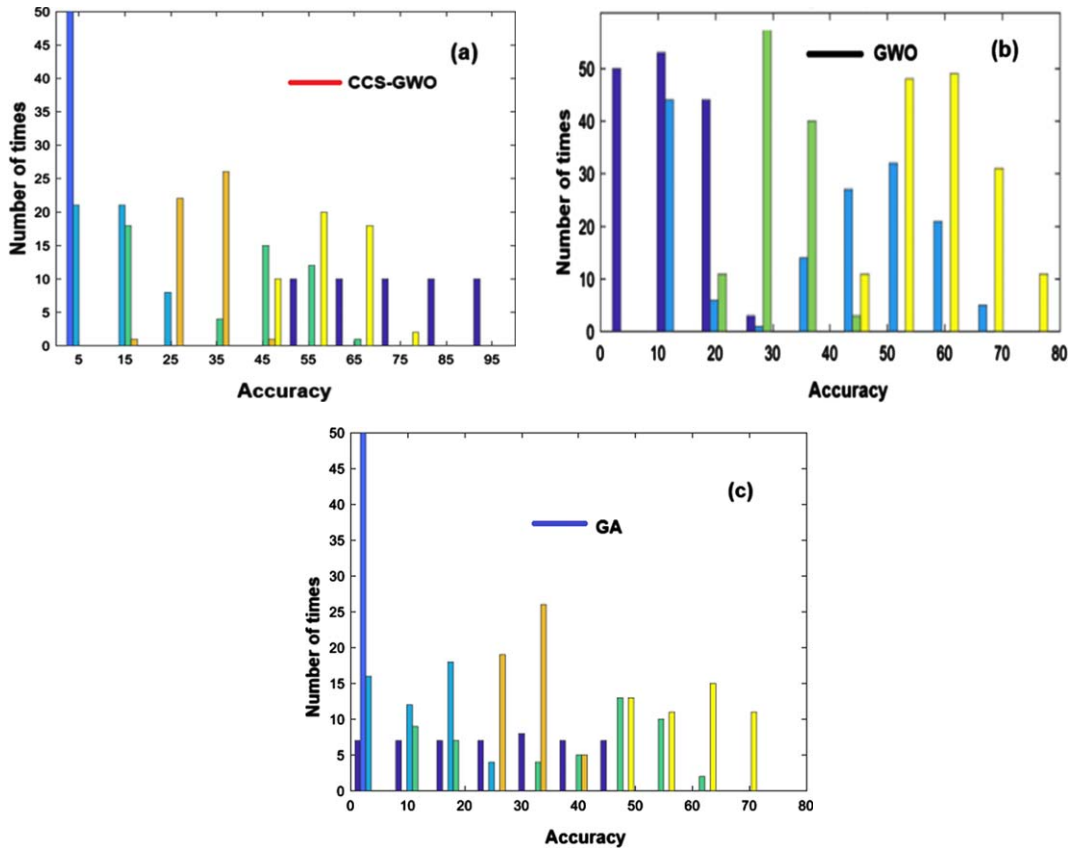


Fig. 14. The CCS-GWO algorithm accuracy (a)GWO algorithm accuracy (b), GA algorithm accuracy (c).

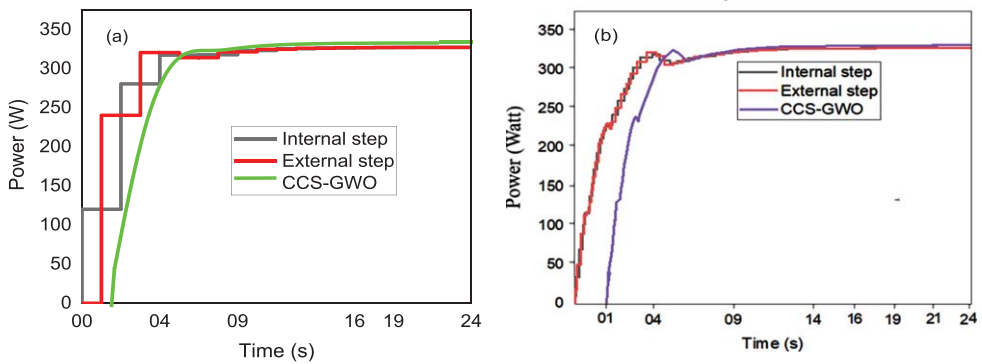


Fig. 15. The CCS-GWO, internal and external step curves (a) under STC and the CCS-GWO, internal and external step curves (b) under partial shading conditions.

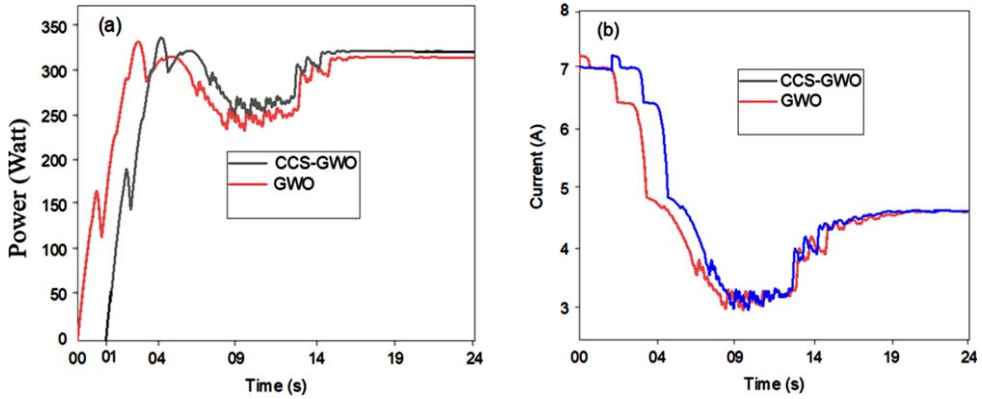


Fig. 16. The CCS-GWO and GWO power curves (a) and the CCS-GWO and GWO current curves (b) under complex partial shading conditions (CPSCs).

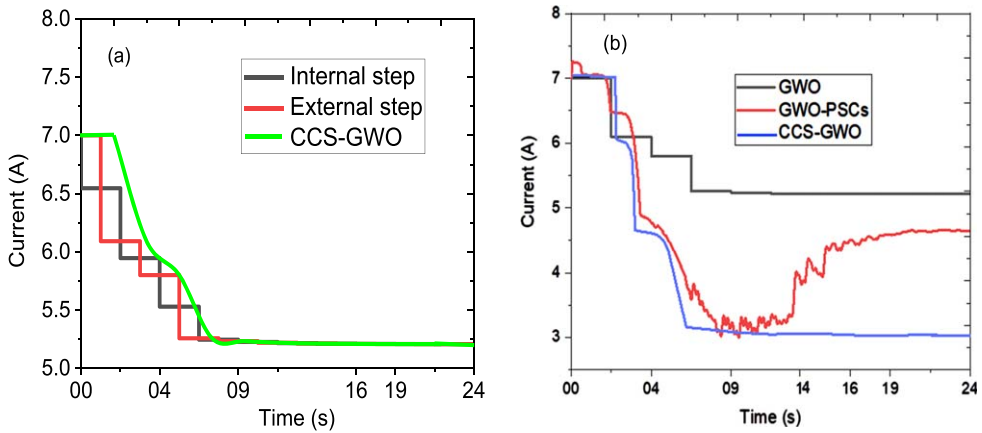


Fig. 17. The CCS-GWO and internal, external step curves (a) at STC and the CCS-GWO, GWO and GWO-PSCs curves (b) under partial shading conditions.

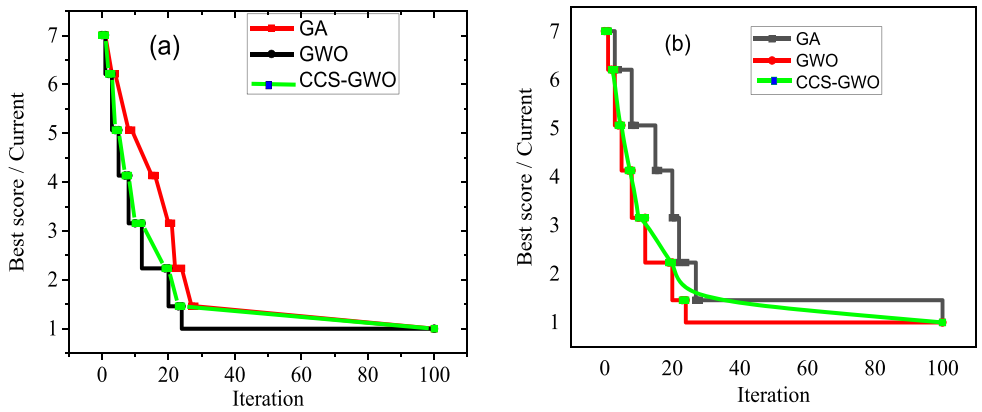


Fig. 18. GA, GWO and CCS-GWO curves (a) and CCS-GWO, internal step and external step curves (b).

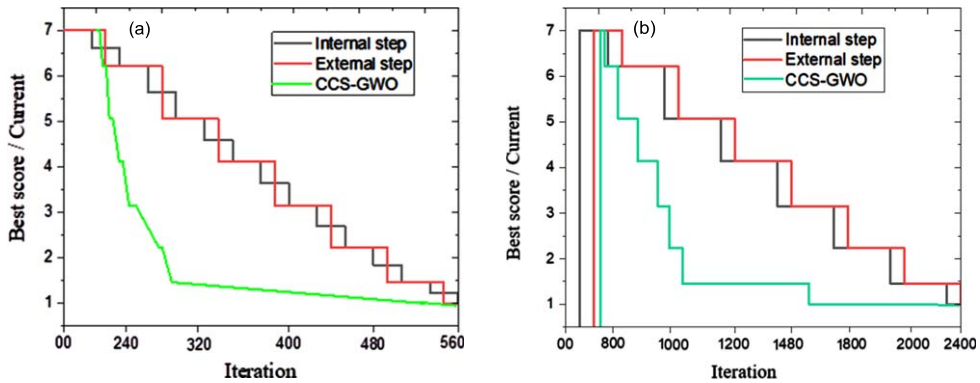


Fig. 19. Adjacent mutation step mode curve (a) and parallel mutation step mode (b) under partial shading conditions.

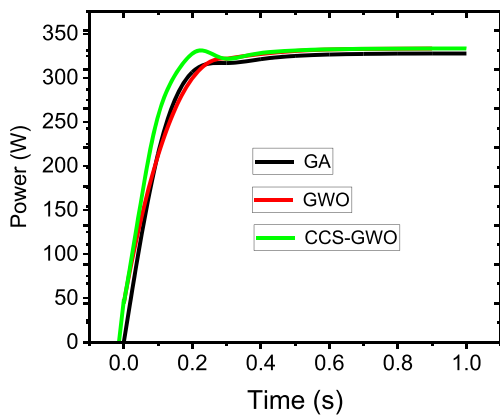


Fig. 20. GA, GWO and CCS-GWO powers curves at STC.

Nomenclature

Abbreviations

GWO	Grey wolf optimization
CCS	Constant current step
STE	Source term estimation
PSCs	Partial shading conditions
MPPT	Maximum power point tracking
GMPP	Global maximum power point
NGWO	Novel grey wolf optimization
AGWO	Adaptive grey wolf optimization
R_s, R_{sh}	Solar cell series and shunt resistance
DLGWO	Dimensional learning grey wolf optimization
Is, es.	Internal step and external step
q	The charge of the electron (C)
T	Absolute temperature ($^{\circ}$ K)
k	Boltzmann constant (J/K)
f_p	Switching frequency

L	Inductance
C	Capacitance

4. Conclusion

This paper suggested an improved constant current step based on the grey wolf optimization (GWO) algorithm abbreviated as CCS-GWO to enhance the inadequate exploration, exploitation, and premature optimum convergence drawbacks of the conventional GWO. A new algorithm is proposed in order to facilitate the mutation sequency and increased hunting performance of the best agents (wolves). The process is done in two steps where the first step (internal step) allows the wolves to converge toward the prey whereas the second step (external step) precludes the wolves from converging toward the prey. By combining these two steps simultaneously or /and in sequencing ways, therefore; convergence speed and efficiency are improved. By applying various climate changes inputs to the proposed CCS-GWO methods, we observed that the new technique outperforms the traditional GWO in terms of mutation accuracy, convergence and exploration (hunting) and performs a good efficiency of 98.55% as compared to 97.10%, and 96.85% for GWO and GA respectively. Besides, the results of the proposed CCS-GWO method for the benchmark functions F5, F11 and F19 presents low standard deviation values of 0.01993, 0.01213, and 0.01331 respectively. Finally, we summarize that the proposed CCS-GWO approach works accurately and tracks the internal steps during the converging process, external steps during the diverging process, combined adjacent internal and external steps, and combined parallel internal and external steps in general cases.

Declarations

Ethical approved

Not applicable for this manuscript.

Competing or conflict of interests

The authors declared no potential conflicts of interest with regards to research, authorship, and/or publication of the article.

Authors' contributions

Idriss Dagal: Design; writing original draft; writing review & editing; funding. Burak Akın: Resources & supervision & Editing. Yaya Dagal Dari: Resources & supervision & Editing.

Acknowledgment

The authors declared that this work does not receive any funding.

Data availability and materials

All data generated or analysed during this study are included in this published article.

References

- [1] L. Bhukya, A. Anil and N. Venkata, A grey wolf optimized fuzzy logic based MPPT for shaded solar photovoltaic systems in microgrids, *International Journal of Hydrogen Energy* **46** (2021), 10653–10665.
- [2] W. Yihao, M. Mingxuan, Z. Lin et al., A Novel Nature-Inspired Maximum Power Point Tracking (MPPT) Controller Based on SSA-GWO Algorithm for Partially Shaded Photovoltaic Systems, *MDPI* **6** (2019), 680.
- [3] A.M. Eltamaly and H.M. Farh, Dynamic global maximum power point tracking of the PV systems under variant partial shading using hybrid GWO-FLC, *Sol. Energy* **177** (2019), 306–316.
- [4] S. Mohanty, B. Subudhi and P.K. Ray, A new MPPT design using grey wolf optimization technique for photovoltaic system under partial shading conditions, *IEEE Trans. Sustain. Energy* **7** (2016), 181–188.
- [5] Y. Hou, H. Gao, Z. Wang and C. Du, Improved grey wolf optimization algorithm and application, *Multidisciplinary Digital Publishing Institute* **22** (2022), 3810.
- [6] Y. Zhang, Modified grey wolf optimization algorithm for global optimization problems, *J. Univ. Shanghai Sci. Technol.* **43** (2021), 73–82.
- [7] M. Wang, Novel grey wolf optimization algorithm based on nonlinear convergence factor, *Appl. Res. Comput.* **33** (2016), 3648–3653.
- [8] L. Rodríguez, O. Castillo, J. Soria, P. Melin, F. Valdez, C.I. Gonzalez, G.E. Martinez and J. Soto, A fuzzy hierarchical operator in the grey wolf optimizer algorithm, *Appl. Soft Comput.* **57** (2017), 315–328.
- [9] S. Saremi, M.S. Zahra and M.S. Mohammad, Evolutionary population dynamics and grey wolf optimizer, *Neural Comput. Appl.* **26** (2015), 1257–1263.
- [10] E. Dada, J. Stephen, O. David and A. Alaba, Application of Grey Wolf Optimization Algorithm: Recent Trends, Issues, and Possible Horizons, *Gazi University Journal of Science* **35** (2021), 485–504.
- [11] S. Lijun, F. Binbin, Z. Tianfei, Z. Dongliang and X. Yan, Equalized grey wolf optimizer with refraction opposite learning, *Computational Intelligence and Neuroscience* **2022** (2022).
- [12] W. Daolei, Y. Jingwei, C. Pingping and H. Feng, Calibration of camera internal parameters based on grey wolf optimization improved by levy flight and mutation, *Scientific Reports* **12**, 1–12.
- [13] Y. Bin, M. Hamza, Mujeeb Khan et al. Improved Hybrid Grey Wolf Optimizer Sine Cosine Algorithm (IHG-WOSCA) Trained Artificial Neural Network (ANN) for Classification. 2021 *16th International Conference on Emerging Technologies (ICET)* (2021), 1–6.
- [14] M. Seyedali, M. Seyed and L. Andrew, Grey wolf optimizer, *Advances in Engineering Software* **69** (2014), 46–61.
- [15] L. Xinyang, W. Yifan and Z. Miaolei, Dimensional learning strategy-based grey wolf optimizer for solving the global optimization problem, *Computational Intelligence and Neuroscience* (2022).
- [16] W. Changging, H. Xiaodong, A. Weiyu and X. Nan, Application of the improved grey wolf algorithm in spacecraft maneuvering path planning, *International Journal of Aerospace Engineering* (2022).
- [17] Adaptive grey wolf optimizer, *Neural Computing and Applications* **34** (2022), 7711–7731.
- [18] Dynamic Grey Wolf Optimization Algorithm Based on Quasi-Opposition Learning. 3D Imaging—Multidimensional Signal Processing and Deep Learning: 3D Images, *Graphics and Information Technologies* **297** (2022), 11.
- [19] E. Isaac, O. Zulkifli and S. Irwan, Optimal design of the grid-connected photovoltaic system using grey wolf optimization, *Energy Reports* **8** (2022), 1125–1132.
- [20] A. Abdullah, I. Al-Kadi and O. Dama, A modified grey wolf optimization algorithm for an intrusion detection system, *Mathematics* **10** (2022), 999.
- [21] W. Xiaojing, S. Chengli, W. Ning and S. Huiyuan, Gray wolf optimizer with bubble-net predation for modeling fluidized catalytic cracking unit main fractionator, *Scientific Reports* **12** (2022), 1–10.
- [22] L. Yizhe, J. Yu, Z. Xin, P. Yong and Q. Yingguam, Combined grey wolf optimizer algorithm and corrected gaussian diffusion model in source term estimation, *Processes* **10** (2022), 1238.
- [23] A. Mohamed, E. Doaa, et al. A new fusion of grey wolf optimizer algorithm with a two-phase mutation for feature selection, *Expert Systems with Applications* **139** (2022), 112824.

- [24] M.M.A. Awan and M.J. Awan, Adapted flower pollination algorithm for a standalone solar photovoltaic system, *Mehran University Research Journal of Engineering and Technology* **41**(4) (2022), 118–127.
- [25] M.M.A. Awan and T. Mahmood, Optimization of maximum power point tracking flower pollination algorithm for a standalone solar photovoltaic system, *Mehran University Research Journal of Engineering and Technology* **39**(2) (2020), 267–278.
- [26] M.M.A. Awan, M.M. and T. Mahmood, A novel ten check maximum power point tracking algorithm for a standalone solar photovoltaic system, *Electronics* **7**(11) (2018), 327.
- [27] M.M.A. Awan and F.G. Awan, Improvement of maximum power point tracking perturb and observe algorithm for a standalone solar photovoltaic system, *Mehran University Research Journal of Engineering & Technology* **36**(3) (2017), 501–510.
- [28] M.M.A. Awan, A.U. Khan, M. Umer, M. Karim and M. Bux, Optimized hill climbing algorithm for an islanded solar photovoltaic system, *Mehran University Research Journal of Engineering and Technology* **42**(2) (2023), 124–132.
- [29] A.M. Eltamaly and H.M.H. Farh, Dynamic global maximum power point tracking of the PV systems under variant partial shading using hybrid GWO-FLC, *Sol. Energy* **177** (2019), 306–316. <https://doi.org/10.1016/j.solener.2018.11.028>.
- [30] S. Mohanty, B. Subudhi, S. Member, P.K. Ray, A Grey Wolf Assisted Perturb & Observe MPPT Algorithm for a PV System **8969** (2016a), 1–8. <https://doi.org/10.1109/TEC.2016.2633722>.
- [31] S. Mohanty, B. Subudhi, P.K. Ray, A new MPPT design using grey Wolf optimization technique for photovoltaic system under partial shading conditions, *IEEE Trans. Sustain. Energy* **7** (2016b), 181–188. <https://doi.org/10.1109/TSTE.2015.2482120>.
- [32] Irfan Yazıcı and K.Y. Ersagun, Modified grey wolf optimizer based MPPT design and experimental performance evaluations for wind energy systems, 2023.
- [33] Ibrahim Saiful Millah et al. An Enhanced Grey Wolf Optimization Algorithm for Photovoltaic Maximum Power Point Tracking Control Under Partial Shading Conditions, 2022.
- [34] Rambabu Motamarri et al. Modified grey wolf optimization for global maximum power point tracking under partial shading conditions in photovoltaic system, 2021.
- [35] Ghazal, Hatem Khalifa Emhmed, Design of a MPPT system based on modified grey wolf optimization algorithm in photovoltaic system under partially shaded condition, 2021.
- [36] E.M. Mohamed Ahmed, et al. Arithmetic optimization algorithm based maximum power point tracking for grid-connected photovoltaic system, 2023.
- [37] M. Valan Rajkumar et al. A New DC–DC Converter Topology with Grey Wolf MPPT Algorithm for Photovoltaic System, 2017.
- [38] Mohamed Abbas et al. Potential Contribution of the Grey Wolf Optimization Algorithm in Reducing Active Power Losses in Electrical Power Systems, 2022.
- [39] Wenxiang Luo et al. MPPT Control Research of Improved Gray Wolf Algorithm According to Levy Flight and Greedy Strategy, 2023.
- [40] M.D. Dieudonné et al. Improvement of the Dynamic Response of Robust Sliding Mode MPPT Controller-Based PSO Algorithm for PV Systems under Fast-Changing Atmospheric Conditions, 2021.
- [41] M.M.A. Awan, A.B. Asghar, M.Y. Javed and Z. Conka, Ordering Technique for the Maximum Power Point Tracking of an Islanded Solar Photovoltaic System, *Sustainability* **15**(4) (2023), 3332.
- [42] M.M.A. Awan, M.Y. Javed, A.B. Asghar and K. Ejsmont, Performance Optimization of a Ten Check MPPT Algorithm for an Off-Grid Solar Photovoltaic System, *Energies* **15**(6) (2022a), 2104.
- [43] M.M.A. Awan, M.Y. Javed, A.B. Asghar and K. Ejsmont, Economic integration of renewable and conventional power sources—A case study, *Energies* **15**(6) (2022b), 2141.
- [44] M.M.A. Awan, A Technical Review of MPPT Algorithms for Solar Photovoltaic System: SWOT Analysis of MPPT, *Sir Syed University Research Journal of Engineering & Technology* **12**(1) (2022c), 98–106.
- [45] M.M.A. Awan and T. Mahmood, Modified flower pollination algorithm for an off-grid solar photovoltaic system, *Mehran University Research Journal of Engineering and Technology* **41**(4) (2022d), 95–105.
- [46] M.M.A. Awan, Strategic perturb and observe algorithm for partial shading conditions: SP&O Algorithm for PSC, *Sir Syed University Research Journal of Engineering & Technology* **12**(2) (2022e), 26–32.
- [47] Hicham Karmouni et al. A Novel MPPT Algorithm based on Aquila Optimizer under PSC and Implementation using Raspberry, 2022.
- [48] Dagal Idriss et al. Atomic Search Optimization Feature Selection for Aircraft Winglet Design, 2023.
- [49] Mustafa Bayasal et al. Microgrid aggregated load short-term forecasting using a Long Short-Term Memory Recurrent Neural Network, 2019a.
- [50] Mustafa Bayasal et al. Phase change material-based heat storage analysis for its integration into renewable microgrid, 2019b.
- [51] Hicham Karmouni et al. Secure and Optimized Satellite Image Sharing based on Chaotic $\epsilon\pi$ Map and Racah Moments, 2023.
- [52] Hou Yuxiang, Gao Huanbing, Wang Zijian and Du Chuan-sheng, Improved grey wolf optimization algorithm and application **22–10** (2022), 3810.
- [53] Wang Jie-Sheng and Li Shu-Xia, An improved grey wolf optimizer based on differential evolution and elimination mechanism **9-1** (2019), 1–21.
- [54] Emmanuel DADA and JOSEPH Stephen and OYEWOLA David, FADELE Alaba Ayotunde et al. Application of grey wolf optimization algorithm: Recent trends, *Issues, and Possible Horizons*. **35–2** (2022), 485–504.
- [55] Gao Zheng-Ming and Zhao Juan, An improved grey wolf optimization algorithm with variable weights **2019** (2019).
- [56] Valenta Daniel and Ciencialov Lucie and Cienciala Ludek, Modelling of grey wolf optimization algorithm using 2D P colonies (2020), 109–122.
- [57] E. Emary and Yamany Waleed, Hassanien Aboul Ella and Snasel Vaclav, Multi-objective gray-wolf optimization for attribute reduction **65** (2015), 623–632.
- [58] Shringi Sakshi and H. Sharma and D.L. Suthar, Fitness-Based Grey Wolf Optimizer Clustering Method for Spam Review Detection **2022** (2022).
- [59] Long Wen and Jiao Jianjun and Liang Ximing and Tang Mingzhu, Inspired grey wolf optimizer for solving large-scale function optimization problems **60** (2018), 112–126.
- [60] Liu ChenYang and Wang Yongli, Grey Wolf algorithm based on S-function and particle swarm optimization **1453–1** (2020), 012–021.

- [61] Natesan Gobalakrishnan and Chokkalingam Arun, An improved grey wolf optimization algorithm-based task scheduling in cloud computing environment **17-1** (2020), 73–81.
- [62] H. Clifford and K. Bruce, Determining Series Resistance for Equivalent Circuit Models of a PV Module, *IEEE Journal of Photovoltaics* **9** (2018), 538–543.
- [63] M. Yousef and X. Weidong, Evaluation of shunt model for simulating photovoltaic modules, *IEEE Journal of Photovoltaics* **8** (2018), 1818–1823.
- [64] S. Sekhar, M. Mahesh and N. Kumar, A Novel Approach for Direct MPP Estimation of a PV Module Under Different Irradiation Conditions, *IEEE Transactions on Energy Conversion* **36** (2021), 3127–3136.
- [65] I. Dagal and B. Akín, Transformer rail-tapped buck-boost converter design-based feedback controller for battery charging systems, *Energy Storage* (2022), e414.
- [66] I. Dagal and B. Akín, Akboy: MPPT mechanism based on novel hybrid particle swarm optimization and Salp Swarm Optimization Algorithm for battery charging through Simulink, *Scientific Reports* **12** (2022), 1–17.
- [67] I. Dagal and B. Akín, Akboy: A novel hybrid series Salp Particle Swarm Optimization (SSPSO) for standalone battery charging applications, *Ain Shams Engineering Journal* **13** (2022), 10174.
- [68] Q. Mohammed, A. Souad, H. Nazar, et al. Large scale salp-based grey wolf optimization for feature selection and global optimization, *Neural Computing and Applications* **34** (2022), 8989–9014.
- [69] S. Mirjalili, S.M. Mirjalili and A. Lewis, Grey wolf optimizer, *Adv. Eng. Soft* **69** (2014), 46–61.
- [70] A.A.Z. Diab and H. Rezk, Optimal sizing and placement of capacitors in radial distribution systems based on the grey wolf, dragonfly, and moth–flame optimization algorithms, *Iranian J Sci Technol Transac Elect Eng.* 1–20.
- [71] S. Mohanty, B. Subudhi and P.K. Ray, A new MPPT design using grey wolf optimization technique for photovoltaic system under partial shading conditions, *IEEE Transac Sustain Energy* **7** (2016), 181–8.
- [72] Q. Li, H. Chen, H. Huang, X. Zhao, Z. Cai, C. Tong, et al. An enhanced grey wolf optimization-based feature selection wrapped kernel extreme learning machine for medical diagnosis, *Computer Mathematical Methods Med* 2017.
- [73] M.A. Mohamed, A.A. Zaki Diab and H. Rezk, Partial shading mitigation of PV systems via different meta-heuristic techniques, *Renew Energy* **130** (2019), 1159–75.
- [74] I. Dagal and B. Akín, Akboy: Improved Salp Swarm Algorithm based on particle Swarm Optimization for maximum power point tracking of optimal photovoltaic systems, *Int J Energy Res.* (2022), 1–18. doi:10.1002/er.7753.